IJPAC : **13(1-2),** *(January-June 2018)*

Synthesis of Bis-Formazan Molecule and Quantum Chemical Calculations

Şakir Erkoç[1*], Habibe Tezcan[2], Emine Deniz Çalişir[1], Figen Erkoç[3]

[1*]*Department of Physics, Middle East Technical University, 06531 Ankara, Turkey.*
[2]*Department of Chemistry Education, Gazi University, 06500 Ankara, Turkey.*
[3]*Department of Biology Education, Gazi University, 06500 Ankara, Turkey.*

ABSTRACT: Bis-formazan molecule has been synthesized experimentally and structural and electronic properties of the bis-formazan molecule have been investigated theoretically by performing semi-empirical molecular orbital (PM3) calculations. The geometry of the molecule has been optimized and the electronic properties and the vibrational spectra of the molecule have been calculated in its ground state.

Keywords: Bis-formazan, semi-empirical PM3 method.

Introduction

Formazans are colored compounds ranging from red to orange or blue depending upon their structures. However they did not have their deserved place in dying industry due to their relatively high cost. There are numerous studies related to formazans such as their synthesis, structure evaluation, photochromic transitions, tautomer formation, redox potentials [1-6] and synthesis of crown formazans [7,8]. Formazans are polydentate ligands with donor atoms and used for analytical purposes for forming complexes with trace metals.

The methods based on reduction of tetrazolium salts are routinely used in biological and biomedical research. It is known that reduction can be catalyzed by intracellular enzymes residing in mitochondria, endoplasmic reticulum, and cytosol as well as oxidoreductases associated with plasma membranes. The formazan/tetrazolium system is described as the marker of vitality. Along this line automated approaches aimed at determining proliferation and survival of cells and screening large numbers of drugs have been designed [9,10-12]. The frequently used formazans in medicine for this purpose are BTT, MTT, XTT and WST-1 [13,14].

* *Corresponding author: Ş. Erkoç, E-mail: erkoc@erkoc.physics.metu.edu.tr*
Tlf.: +90 312 210 32 85
Fax: +90 312 210 12 81

Capacity of a tetrazolium salt to cross intact plasma membranes constitutes an important experimental variable which needs to be controlled in order to correctly interpret the outcome of tetrazolium assays designed to measure cellular production of oxygen and superoxide radicals, activity of mitochondrial, cytosolic, or outer membrane reductases, measurements of activity of oxidoreductases, subcellular localization of oxidoreductases, detection of superoxide radicals, testing of cell viability and growth, and mycoplasma screening [14]. In a study using the formazan dye containing a nitro group, metal-complex formation using iron increased mutagenicity in the Salmonella bioassay [15]. Quantitative formazan production from tetrazolium salt XTT was used to detect the antiproliferative properties of antiviral drugs by prevention of the cytopathic effects of HIV in cultures of the target cells used [13].

Recently a new rapid screening method for glucose-6-phosphate dehydrogenase (G6PD) deficiency diagnosis was described based on a method incorporating a new formazan substrate (WST-8) and capable of detecting heterozygous females both qualitatively and quantitatively. The new, rapid screening method may be essential for the diagnosis of G6PD deficiency particularly in rural areas without electricity, and can be recommended for use in malaria control programmes [16].

Another widely used application is in microbiology. Use of the redox dye 5-cyano-2,3,-ditolyl tetrazolium

chloride (CTC) for evaluating the metabolic activity of aerobic bacteria has gained wide application in recent years. Bhupathiraju et al. examined the utility of CTC in capturing the metabolic activity of anaerobic as well as aerobic bacteria [9]. Anaerobic bacterial cells also accumulated intracellular CTC-formazan crystals during the exponential phase of growth. CTC-formazan production by all cultures examined was proportional to biomass production. The highly colored, water insoluble formazans formed by reduction of tetrazolium salts have been developed for utilization in radiation processing dosimetry [17].

Study of formazans by mass spectrometry showed the protonated formazans to be relatively unstable, decomposing through several fragmentation pathways. Regardless of the reagent gas, the decomposition was always of the same degree and the spectra were closely similar. The most probable protonation site for the formazans was estimated by semi-empirical calculations to be the benzothiazole nitrogen. This result is in agreement with the experimental data both under EI and CI, and showed that those tautomeric forms of formazans having a single bond between C3 and N4 are dominant in the gas phase [18]. The only theoretical studies on formazan molecular structure are: formazan and 3-nitroformazan at ab initio level [19] and 1,3,5-triphenylformazan [20] using density functional theory (DFT).

The various synthesized formazans have electron donating and withdrawing groups attached to the 1-phenyl [21,22] and 3-phenyl rings [23,24]. Determination of active/live cells is based on the presence and the amount of the formazan where better light absorbing substituents will improve sensitivity of the test system.

The bis-formazan molecule has been synthesized with the aim of obtaining a less toxic and more suitable derivative for biomedical applications. We report quantum chemical study of bis-formazan for the first time in this study. The experimental procedure and results obtained for the bis-formazan molecule, and the theoretical features of the bis-formazan molecule have been discussed seperately.

Experimental

In this study, 1,4-bis-[3,3'-pheny l-5,5'-(2-carboxyphenyl)-formaz-1-yl]-benzene-2-sulphonic acid (bis-formazan, CSPF) was synthesized. The structure of the formazan thus obtained was elucidated by elemental analysis, Mass spectroscopy, IR, ^{1}H-NMR and UV-Vis spectra.

The ^{1}H-NMR spectrum of the formazan synthesized was measured on a BRUKER 400 MHz ^{1}H-NMR spectrometer using 10^{-4} M solution in $CDCl_3$. The IR spectrum was recorded with the use of MATTSON 100 FT-IR spectrometer, using KBr pellet in the range of 4000-400 cm^{-1}. The UV-Vis spectrum was obtained with UNICAM UV2-100 UV-visible spectrometer in 1 cm quartz cell, in 10^{-4} M methanol solution using 325 nm UV lamb. Elemental analysis was carried out by means of a CHNS-932 LECO device and electron impact mass spectrum was taken on a UK Platform-II micromass spectrometer at 70 eV.

Synthesis of CSPF

Benzaldehyde (2.12 g, 2.04 ml, 0.02 mol) was diluted with methanol (40 ml). 2-Hydrazynobenzoic acid (3.76 g, 0.02 mol) was dissolved in a mixture of methanol (80 ml) and water (20 ml). 2-Hydrazynobenzoic acid solution was added to the benzaldehyde solution with constant stirring in dropwise fashion adjusting the pH value to 5-6. A light yellow colored benzaldehyde-2-carboxyphenyl hydrazone precipitated out. The product is recrystallized from methanol-water mixture. This hydrazone was dissolved in methanol (75 ml) water (25 ml) mixture under reflux. On the other side the basic buffer solution was prepared by dissolving NaOH (2.50 g) and sodium acetate (3.50 g) in 200 ml methanol under reflux and added to the hydrazone solution as prepared above. This basic buffer and hydrazone solution mixture was cooled down to –5°C for the coupling reaction (stock solution).

On the other hand the 2-sulphobenzen-1,4-di-diazonium chloride solution was prepared with 2,5-diaminobenzen sulphonic acid (1.88g, 0.01 mol) concentrated HCl (5 ml) and $NaNO_2$ (1.40g, 0.02 mol) in usual way at -5° – 0°C. This diazonium chloride solution was added in drop wise manner to basic buffer-hydrazone solution (stock solution) which was cooled down to -5° – 0°C with constant stirring. Stirring was continued for two hours at the same temperature for the coupling reaction. Care was taken for the temperature not to exceed -5° – 0°C. The pH was approximately adjusted to 6 by the addition of HCl for the precipitation of the product. The mixture was kept in the refrigerator at the same temperature for five days. The red colored formazan precipitated out. The product was recrystallized from methanol-water-dioxin mixture. Yield: 55%; red crystals; m.p. 255° – 256°C.

Molecular formula of the synthesized material was $C_{34}H_{26}O_7N_8S$. (MW 690.30; Elementary analysis calculated: C 59.13% H 3.76% N 16.23% S 4.63%, found: C 59.01% H 3.67% N 16.12% S 4.68%). Spectral analysis: MS (EI, 70 eV): m/z (%) = 690.12 (0.51) [M^+]; 658 (2.21); 599 (5.27); 520 (11.48); 300 (47.25); 255 (78.89); 240 (67.33); 188 (22.64).

The NMR data are tabulated in Table 1. UV-Visible absorption λ_{max} values are given in Table 2. The IR (KBr) spectral data are given in Table 3. Considering all these experimental findings we have predicted structure of the synthesized bis-formazan molecule as shown in Figure 1. The experimental IR spectrum of the bis-formazan molecule (CSPF) is displayed in Figure 2.

Table 1
The ^{1}H-NMR data of CSPF (bis-formazan)
(400 MHz, in $CDCl_3$, δ in ppm)

Comp.	*Ar-H*	*N-H*	*COOH*	*SO_3H*
CSPF	8.55-6.90 (m,21H)	2.50-2.25 (s,2H)	10.90 (s,2H)	11.28 (s,1H)

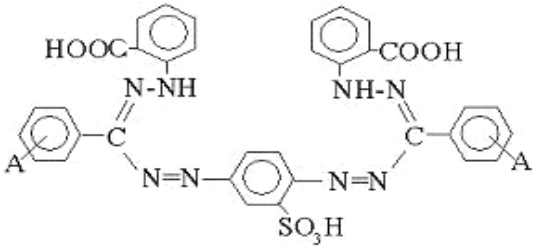

Figure 1: Experimentally predicted structure of the bis-formazan molecule.

Method of Calculation

In the present study, the bis-formazan molecule in the gas phase, namely an isolated bis-formazan molecule, has been investigated theoretically by performing semi-empirical molecular orbital calculations. Preoptimization has been performed by applying the molecular-mechanics (MM) method [25] using MM+ force field [26]; this makes easier to perform full optimization by extended methods. Semi-empirical self-consistent-field molecular-orbital (SCF-MO) method at PM3 level [27] within the restricted Hartree-Fock (RHF) [28] formalism has been considered to optimize fully the geometry of the bis-formazan molecule in its ground state.

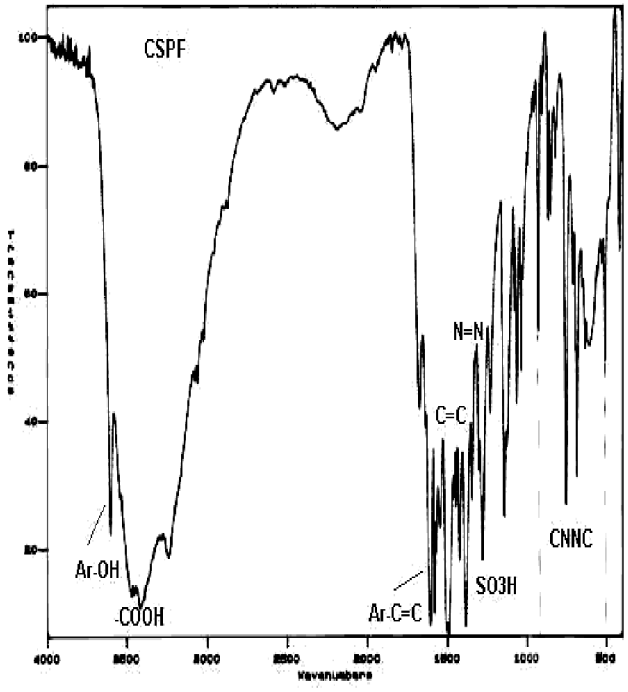

Figure 2: Experimental IR (KBr) spectra of the bis-formazan molecule (CSPF)

Table 2: UV-Visible absorption spectra λ_{max} values of bis-formazan (CH_3OH, 10^{-4} $molL^{-1}$).

Comp.	*λ_{max1}(nm) (Abs)*	*λ_{max2}(nm) (Abs)*	*λ_{max3}(nm) (Abs)*
CSPF	498 (0.762) (formazans' peak)	352 (0.912)	233 (0.565)

Geometry optimization is carried out by using a conjugate gradient method (Polak-Ribiere algorithm [29]), then the electronic structure and the vibrational spectra (infrared spectra) of the system have been calculated. The SCF convergency is set to 0.001 kcal/mol and the RMS gradient is set to 0.003 kcal/(Å mol) in the calculations. We have performed all the calculations by using the HyperChem-7.5 packet program [30].

Table 3
The IR spectral data of bis-formazan (KBr, cm^{-1})

Comp.	*C=C stretching*	*N=N stretching*	*Aromatic C=C stretching*	*CNNC Skeletal vibration*	*Ar-OH stretching*	*-COOH stretching*	*-SO_3H stretching*
CSPF	1540-1580	1455-1335	1629	930-600	3600	3400-3300	1420-1330

Results and Discussion

The molecular formula of the bis-formazan molecule is $C_{34}H_{26}N_8O_7S$. The geometry optimization of PM3 method yields a 3D structure as the stable form with C_1 symmetry for the isolated bis-formazan molecule. The optimized geometry of the bis-formazan molecule is shown in Figure 3. The optimized structures of bis-formazan molecule with respect to both MM and PM3 methods are not the same. The MM optimized structure of bis-formazan is almost planar; however the PM3 optimization has changed the MM optimized structure as shown in Figure 3.

PM3 method considers 250 electrons, 125 doubly occupied levels, and 226 total number of orbitals for the bis-formazan molecule. Some of the calculated molecular properties of the bis-formazan molecule are given in Table 4. The bond lengths and the calculated excess charge on the atoms of the bis-formazan molecule are shown in Figures 4 and 5, respectively. The highest occupied and the lowest unoccupied molecular orbital energies (HOMO and LUMO, respectively), and the frontier molecular orbital energy gap (HOMO-LUMO energy difference, E_g) with the calculated dipole moment value of the system considered are also given in Table 4. The MO eigenvalue spectrum and the vibrational spectrum (IR spectrum) with corresponding integrated infrared band intensities are shown in Figure 6. 3D plots of HOMO and LUMO are presented in Figure 7. 3D charge distribution and electrostatic potential plots are displayed in Figure 8.

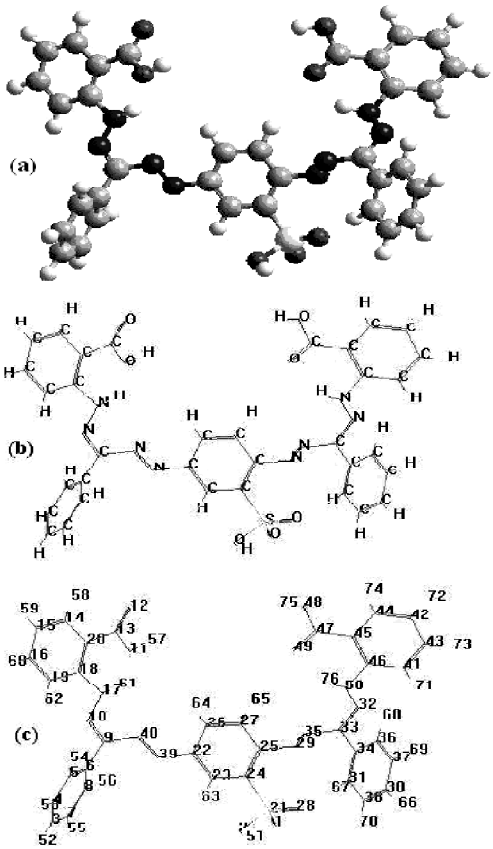

Figure 3: The optimized structure of the bis-formazan molecule. The structure of bis-formazan has C_1 symmetry in its ground state; optimization has been performed by PM3 method. Panel (a) shows the ball and stick model picture of the optimized structure of the bis-formazan molecule. Panel (b) shows the atomic labels, and panel (c) shows the number labels of the atoms of the bis-formazan molecule.

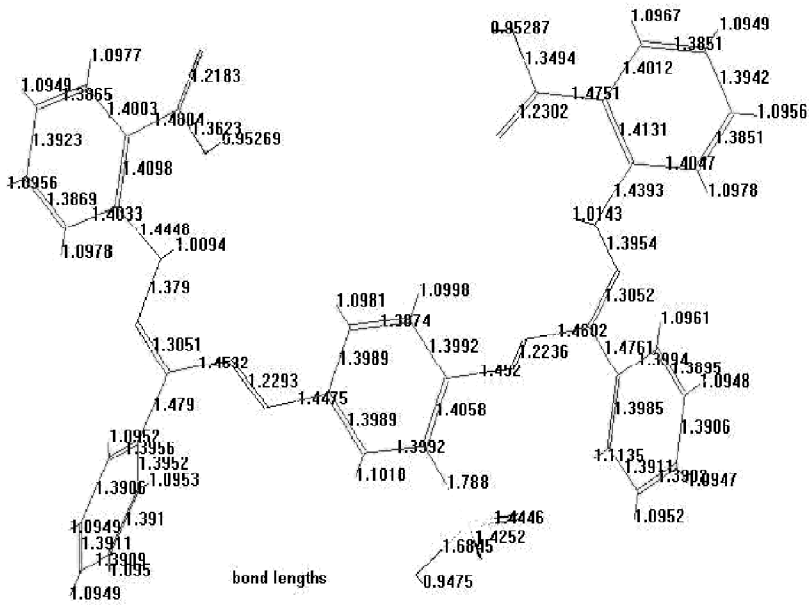

Figure 4: Bond lengths (in Angstrom) of the bis-formazan molecule.

Table 4
Some of the Calculated Molecular Properties and Energy values (in kcal/mol unless otherwise stated) of the Bis-Formazan Molecule (according to PM3 method).

Quantity	*value*	*Quantity*	*value*
Surface area (Å^2)	852.29	Total Energy	-183619.046
Volume (Å^3)	1780.82	Binding Energy	-8551.972
Hydration energy	-33.20	Isolated Atomic Energy	-175067.074
log P	2.30	Electronic Energy	-1882440.833
Refractivity (Å^3)	209.75	Core-Core Interaction	1698821.786
Polarizability	68.33	Heat of Formation	0.253
Mass (amu)	690.69	HOMO (eV)	-8.646
Dipole moment (Debye)	3.437	LUMO (eV)	-1.512
Zero point energy of vib.	350.663	E_g (eV)	7.134

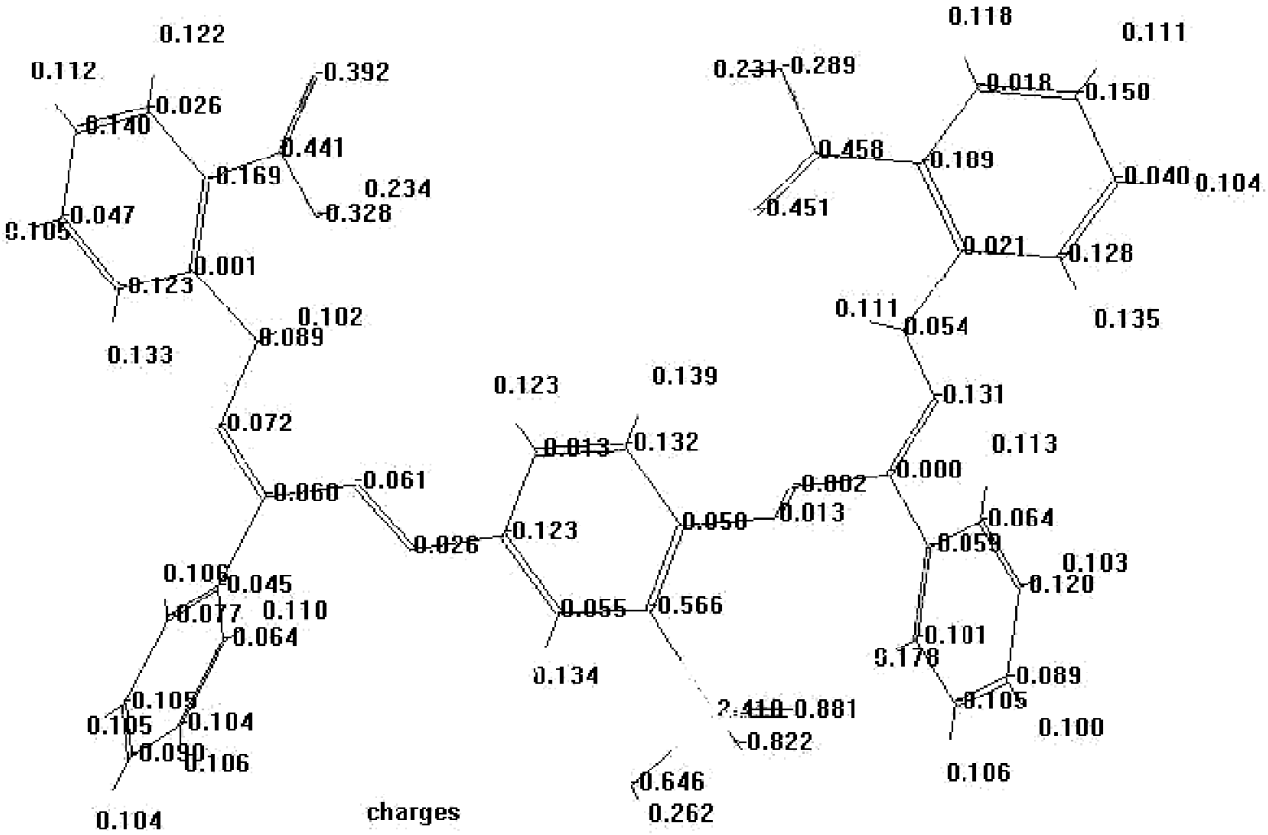

Figure 5: Excess charge (in units of electron charge *e*) on atoms of the bis-formazan molecule.

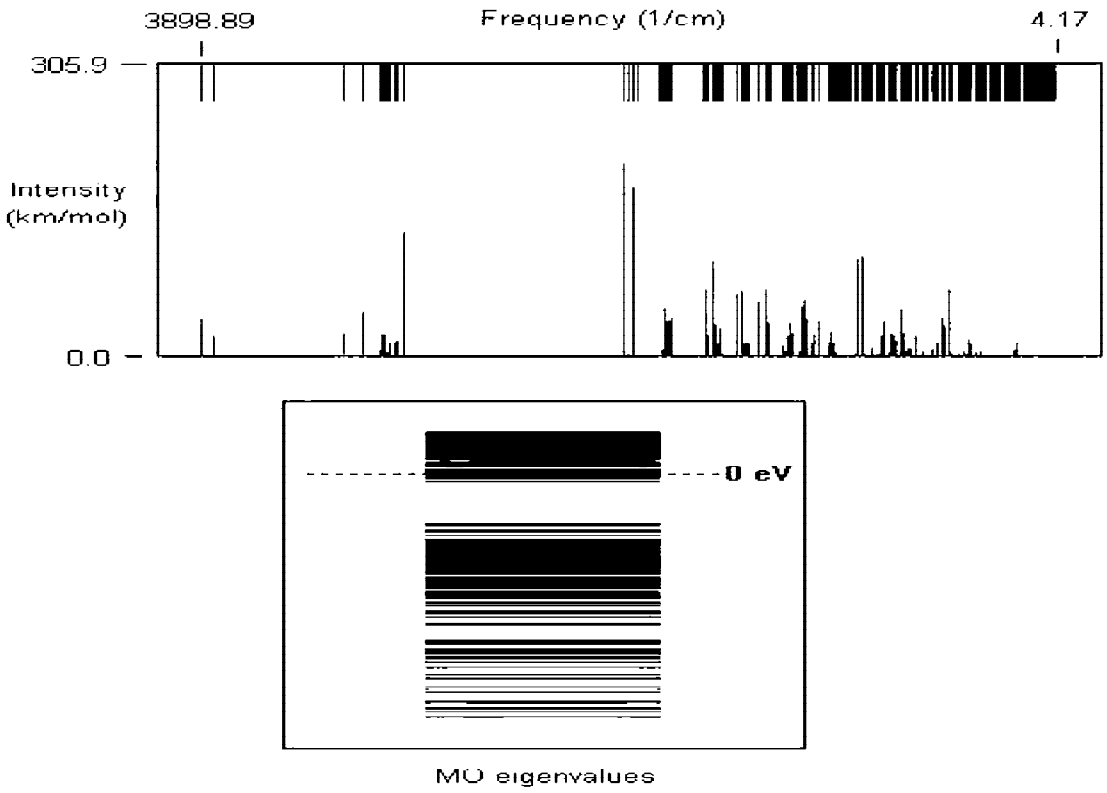

Figure 6: Vibrational spectra (frequencies and intensities) and MO eigenvalue spectrum of the bis-formazan molecule.

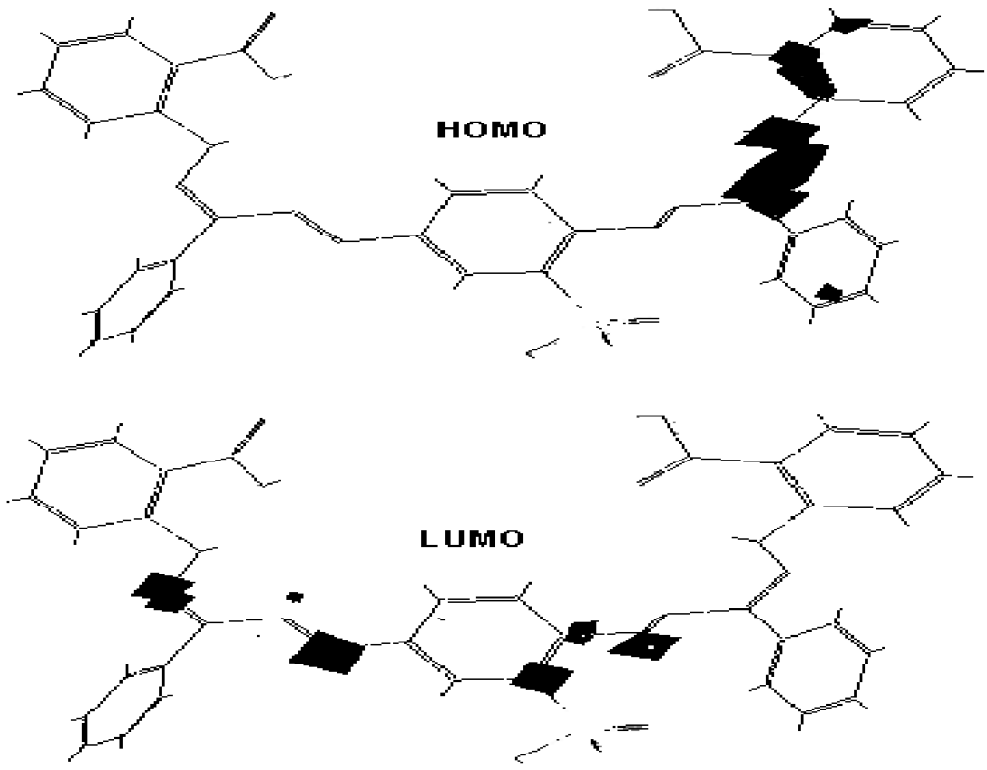

Figure 7: 3D HOMO and LUMO plots of the bis-formazan molecule.

According to PM3 calculation binding energy of the bis-formazan molecule is about-8552 kcal/mol, heat of formation of bis-formazan is about 0.253 kcal/mol and it is endothermic. On the other hand, according to PM3 calculation frontier molecular orbital energy gap, namely the HOMO-LUMO gap, E_g of the bis-formazan molecule is about 7 eV. The bis-formazan molecule has a dipole moment of about 3.4 Debyes. According to the present calculated dipole moment value, bis-formazan molecule seems to be polar (hydrophilic). This property of bis-formazan makes it an active molecule with its environment that is bis-formazan molecule may interact with its environment strongly in solution.

According to PM3 calculation charge distribution shows an interesting feature; the maximum positive excess charge accumulation is on the sulfur atom (about +2.41*e*), on the other hand, the maximum negative excess charge accumulation appears on the oxygen atom (atom label # 28, bonded to S atom, which has excess charge of about -0.88*e*). Oxygen atoms have considerable amount of negative excess charge. Charge accumulation on nitrogen atoms are very small (varying in the range -0.07 – +0.09). Oxygen atoms in the bis-formazan molecule may play an important role in structure activity relationships. This feature also appears in electrostatic potential plot (see Figure 8).

Again according to PM3 calculations, another interesting feature appears in the localization of HOMO and LUMO. HOMO is localized mainly on the atoms C32, N50, N46, C45. However, LUMO is localized mainly on the atoms N29, C24, N39, N10. LUMO is distributed on almost the central part of the molecule; whereas HOMO is distributed on one of the branches of the molecule (see Figure 3 for labels). This HOMO-LUMO localization on the bis-formazan molecule may show interesting spectroscopic properties, especially in electronic spectra.

According to PM3 calculations the vibrational spectra (infrared spectra) of the bis-formazan molecule (as shown in Figure 6) show an interesting feature. There are 222 normal modes of vibrations, the first three normal modes with maximum integrated infrared band intensities have frequencies of ~ 1976, 1925, and 2976 cm^{-1}, the corresponding integrated infrared band intensity values are, respectively, ~ 204, 179, and 132 km/mol. These normal mode frequencies belong to the vibrations, respectively: (C13-O12 bond stretchings); (C47-O49 bond stretching); and (C33-C34-C31-C38 torsion angle). The calculated IR spectra (Figure 6) qualitatively agree with the experimentally obtained one (Figure 2).

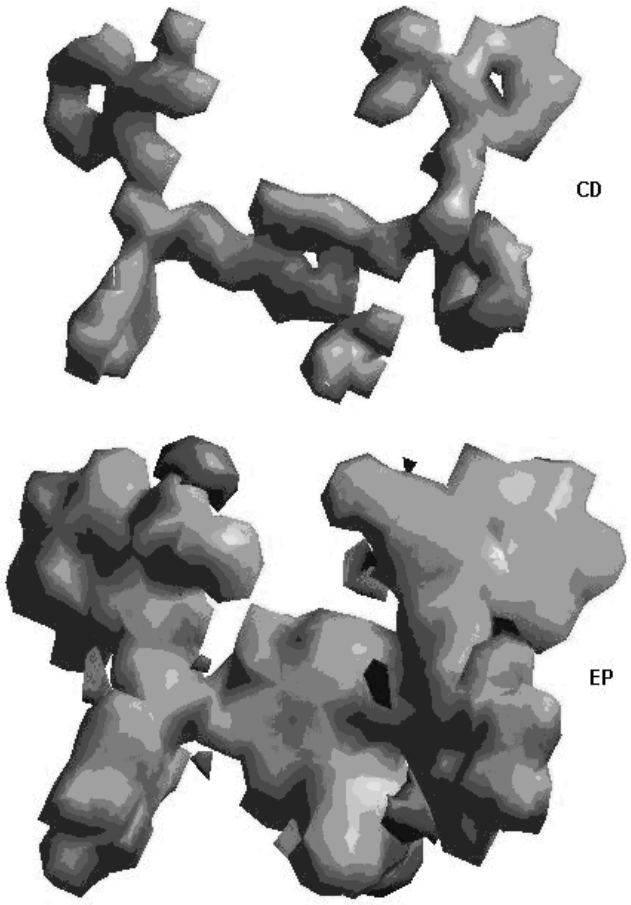

Figure 8: 3D charge density distribution and electrostatic potential plots of the bis-formazan molecule.

Acknowledgements

The authors (Ş.E. and E.D.Ç.) would like to thank METU for partial support through the project METU-BAP-08-11-DPT-2002-K120-510 and (F.E.) would like to thank Gazi University for partial support through the project GAZI-BAB-04/2004-14.

REFERENCES

[1] L. Hunter, C.B. Roberts, The Associating Effect of the Hydrogen Atom. Part IX. The N- H-NBond. Virtual Tautomerism of the Formazyl Compounds, *J. Chem. Soc.* 9 **(1941)** 820-823.

[2] A.M. Mattson, C.O. Jensen, R.A. Dutcher, The preparation of 2,3,5-triphenyltetrazolium chloride, *J. Am. Chem. Soc.* 70 **(1948)** 1284-1284.

[3] G. Arnold, V.C. Schiele, IR Spektroskopische Untersuchungen am System Tetrazoliumsalz-Formazan-III. IR-Spektren von Triarylformazanen im Bereich von, Spectrochlinica Acta 25 **(1969)** 685-696.

[4] V.C. Schiele, IR-und UV-VIS-Spektroskopische

Untersuchungen am System Tetrazoliumsalz/Formazan, Berichte der. Bunsengesellschaft, 30 **(1964)** 308-318.

[5] J.W. Lewis, C. Sandorfy, Infrared-absorption and resonance raman-scattering of photochromic triphenylformazans, *Can. J. Chem.* 61 **(1983)** 809-816.

[6] A.R. Katritzky, S.A. Belyakov, D. Cheng, H.D. Durst, Synthesis of formazans under phase-transfer conditions, Synthesis-Stuttgart 5 **(1995)** 577-581.

[7] Y.A. Ibrahim, A.H.M. Elwahy, A.A. Abbas, New synthesis of macrocyclic crown-formazans from pyruvic-acid derivatives, Tetrahedron 50 **(1994)** 11489-11498.

[8] A.A. Abbas, New synthesis of 28- and 30-crown-formazans and bis formazans, Tetrahedron 54 **(1998)** 12421-12428.

[9] V.K. Bhupathiraju, M. Hernandez, D. Landfear, L. Alvarez-Cohen, Application of a tetrazolium dye as an indicator of viability in anaerobic bacteria, *J. Microbiol. Met.* 37 **(1999)** 231-243.

[10] T. Bernas, J. Dobrucki, Reduction of a tetrazolium salt, CTC, by intact HepG2 human hepatoma cells: subcellular localisation of reducing systems, Biochim. Biophys. Acta 1451 **(1999)** 73-81.

[11] S.A. O'Toole, B.L. Sheppard, E.P.J. McGuinness, N.C., Gleeson, M. Yoneda, J. Bonnar, The MTS assay as an indicator of chemosensitivity/resistance in malignant gynaecological tumours, Cancer Detec. Preven. 27 **(2003)** 47-54.

[12] T. Bernas, J. Dobrucki, Mitochondrial and nonmitochondrial reduction of MTT: Interaction of MTT with TMRE, JC-1, and NAO mitochondrial fluorescent probes, Cytometry 47 **(2002)** 236-242.

[13] H. Elo, The antiproliferative agents trans-bis (resorcylaldoximato) copper(II) and trans-bis (2,3,4-trihydroxybenzaldoximato) copper(II) and cytopathic effects of HIV, Z. Naturforsch. C- J. Biosci. 59 **(2004)** 609-611.

[14] T. Bernas, J.W. Dobrucki, The role of plasma membrane in bioreduction of two tetrazolium salts, MTT, and CTC, Arch. Biochem. Biophys. 380 **(2000)** 108-116.

[15] L.C. Edwards,H.S. Freeman, L.D. Claxton, Developing, azo and formazan dyes based on environmental considerations: Salmonella mutagenicity, Mutat. Res. 546 **(2004)** 17-28.

[16] A. Jalloh, I.S. Tantular, s. Pusarawati, A.P. Kawilarang, H. Kerong, K. Lin, M.U.Ferreira, H. Matsuoka, M. Arai, K. Kita, F. Kawamoto, Rapid epidemiological assessment of glucose-6-phosphate dehydrogenase deficiency in malaria-endemic areas in Southeast Asia using a novel diagnostic kit, Trop. Med. Int. Health 9 **(2004)** 615-623.

[17] A. Kovacs, M. Baranyai, L. Wojnarovits, I. Slezsak, W.L. McLaughlin, A. Miller, A. Moussa, Dose determination with nitro blue tetrazolium containing radiochromic dye films by measuring absorbed and reflected light, Radiat. *Physics Chem.* 57 **(2000)** 711-716.

[18] J.M.J. Nuutinen, P. Vainiotalo, Electron ionization and chemical ionization mass spectrometric studies on 2-benzothiazolphenylhydrazones and1-(2-benzothiazolyl) -3,5- diphenylformazans, Rapid Commun. Mass Spec. 12 **(1998)** 1691-1696.

[19] G. Buemi, F. Zuccarello, P. Venuvanalingam, M. Ramalingam, S.S.C. Ammal, Ab initio study of formazan and 3-nitoformazan, *J. Chem. Soc. Faraday Trans.* 94 **(1998)** 3313–3319.

[20] R.A. King, B. Murrin, A computational study of the structure and synthesis of formazans, *J. Phys. Chem.* A 108 **(2004)** 4961–4965.

[21] H. Tezcan, T. Uyar, The effects of electron donating substituents on UV-Visible absorption spectra of 1,3,5-triphenylformazans, Turkish J. Spectroscopy (Ege Univ.) 9 **(1988)** 8–19.

[22] H. Tezcan, T. Uyar, R. Tezcan, The effect of electron withdrawing substituents on UV absorption spectra of 1,3,5-triphenylformazans, Turkish J. Spectroscopy (Ege Univ.) 10 **(1989)** 82-90.

[23] H. Tezcan, S. Can, R. Tezcan, The synthesis and spectral properties determination of 3-substituted pheny l-1,5-diphenylformazans, Dyes and Pigments 52 **(2002)** 121-127.

[24] H. Tezcan, N. Ozkan, Substituent effects on the spectral properties of some 3-substituted formazans, Dyes and Pigments 56 **(2003)** 159-166.

[25] U. Burkert, N.L. Allinger, Molecular Mechanics (ACS Monograph 177, 1982).

[26] N.L. Allinger, Conformational analysis 130. MM2. A hydrocarbon force field utilizing V_1 and V_2 torsional terms, *J. Am. Chem. Soc.* 99 **(1977)** 8127-8134.

[27] J.J.P. Stewart, Optimization of parameters for semi-empirical methods I. Method, *J. Comput. Chem.* 10 **(1989)** 209-220.

[28] C.C.J. Roothaan, New developments in molecular orbital theory, *Rev. Mod. Phys.* 23 **(1951)** 69-89.

[29] P. Fletcher, Practical Methods of Optimization (Wiley, 1990).

[30] Hypercube, Inc., Gainesville, FL, USA.